Optimal Behavior of a Hybrid Power Producer in Day-Ahead and Intraday Markets

A Bi-Objective CVaR-Based Approach

Khaloie, Hooman; Mollahassani-pour, Mojgan ; Anvari-Moghaddam, Amjad

Published in:
I E E E Transactions on Sustainable Energy

DOI (link to publication from Publisher):
10.1109/TSTE.2020.3026066

Publication date:
2021

Document Version
Accepted author manuscript, peer reviewed version

Optimal Behavior of a Hybrid Power Producer in Day-Ahead and Intraday Markets: A Bi-Objective CVaR-Based Approach

Hooman Khaloie, Mojgan Mollahasani-Pour, and Amjad Anvari-Moghaddam, *Senior Member, IEEE*

***Abstract*—Coordinated operation of various energy sources has drawn the attention of many power producers worldwide. In this paper, a Concentrating Solar Power Plant (CSPP) along with a wind power station, a Compressed Air Energy Storage (CAES) unit, and a Demand Response Provider (DRP) constitute the considered Hybrid Power Producer (HPP). In this regard, this paper deals with the optimal participation of the mentioned HPP in the Day-Ahead (DA) and intraday electricity markets by benefiting from the joint configuration of all accessible resources. To attain risk-averse strategies in the suggested model, Conditional Value-at-Risk (CVaR) based on the ϵ-constraint technique is employed, while its efficiency is validated compared to the previously applied method to such problems. On the whole, the main contributions of this work lie in: 1) proposing a novel model for optimal behavior of a CSPP-based HPP in DA and intraday markets using a three-stage decision-making architecture, and 2) developing a bi-objective optimization framework to improve the functioning of the risk-constrained algorithm. Simulation results reveal that taking advantage of the CSPP in the intraday market and coordinated operation of all resources not only enhance the profitability of the system but also lessen the associated risk compared to the previous models.**

***Index Terms*—Compressed Air Energy Storage (CAES), Concentrating Solar Power Plant (CSPP), Demand Response Provider (DRP), wind farm, stochastic programming, ϵ-constraint method.**

Nomenclature

Indices and superscripts

b	Linearized segment index.
CA/CS	Index of the CAES/ CSPP variables.
ch/dis	Charging/ Discharging mode index.
D	Day-Ahead market index.
HPP	Index of the HPP variables.
I	Intraday market index.
$N_b/N_t/N_\Omega$	Set of the linearized segment/ time/ scenario.
s	Simple-Cycle mode index.
t	Time index.
WF	Index of the wind farm variables.
ω	Scenario index.

Parameters

c	Scale factor of the wind speed in the Rayleigh distribution.
CP^{co}/CP^{exp}	Maximum participation capacity of the CAES in compressing/ expanding status [MW].
CP^{CS}/CP^{WF}	Maximum participation capacity of the CSPP/ wind farm [MW].
$CP^{I,HPP,buy/sell}$	HPP's maximum buying/ selling capacity in the intraday market [MW].
EC^{Max}	Maximum level of the scheduled energy in the CAES [MWh].
ER	Energy conversion rate in the cavern of the CAES [%].
GP	Price of natural gas [€/MBtu].
Htr	Heat rate of the CAES in an operating mode [MBtu/MWh].
j	Grid point number in the ϵ-constraint method.
L_0	Initial load [MW].
OM^{co}/OM^{exp}	Maintenance and operation cost in compressing/ expanding status of the CAES [€/MWh].
$Q^{E,Min}/Q^{E,Max}$	Minimum/ Maximum bounds of the utilized thermal power in the CSPP [MW].
$Q^{S,Min}/Q^{S,Max}$	Minimum/ Maximum capacity of the thermal energy storage in the CSPP [MWh].
RD^{ch}/RD^{dis}	Ramp down rate for charging/ discharging of the thermal energy storage in the CSPP [MW/h].
RU^{ch}/RU^{dis}	Ramp up rate for charging/ discharging of the thermal energy storage in the CSPP [MW/h].
S	Slope of blocks in a linearized curve.
α/β	A parameter designating the confidence/ risk-aversion degree with $\alpha/\beta \in (0,1)$.
Γ	Rate of resources contribution in the intraday market.
δ	Accepted rate of DRP's load curtailments in a period based upon its loading.
κ^{price}	Mean value of electricity market prices in the normal distribution [€/MWh].
λ_1	Conversion efficiency of thermal power to the electric one via the solar field in the CSPP [%].
λ_2	Efficiency of converting the thermal energy of the solar field and conveyed to the thermal energy storage in the CSPP [%].
λ_3	Conversion efficiency of thermal power to the electric one via the thermal energy storage in the CSPP [%].
μ	Accepted rate of DRP's load curtailments in the entire time horizon based upon its total loading.
π_ω	Occurrence probability of scenario ω.
σ^{price}	Standard deviation of electricity market prices in the normal distribution [€/MWh].
Υ	Correlation factor between load and electricity price.
φ^*	Incentive of the DRP [€/MWh].

Variables

H. Khaloie is an Independent Researcher, Kerman, Iran (e-mail: hoomankhaloiee@gmail.com).

M. Mollahasani-Pour is with the Faculty of Electrical and Computer Engineering, University of Sistan and Baluchestan, Zahedan, Iran (m.mollahassani@ece.usb.ac.ir).

A. Anvari-Moghaddam (corresponding author) is with the Department of Energy Technology, Aalborg University, 9220 Aalborg East, Denmark (e-mail: aam@et.aau.dk).

CL^I/CL^D	Load curtailment offer of the DRP in the DA/ intraday market [MW].
CL^{Sch}	Scheduled load curtailment offer of the DRP [MW].
EC^{CA}	Scheduled energy in the CAES [MWh].
ESF	The produced thermal power via the solar field [MW].
PW	Generated power of the wind farm [MW].
Q^{FE}	Thermal power from the solar field employed to produce power in the CSPP [MW].
Q^{FS}	Transferred thermal power from the solar field to the storage in the CSPP [MW].
Q^S	Amount of the stored energy in the thermal energy storage device [MWh].
Q^{SE}	Thermal power from thermal energy storage employed to produce power in the CSPP [MW].
r^-/r^+	Imbalance ratio for negative/ positive energy deviation.
u	Commitment status of the CAES in any of charging, discharging, and simple-cycle modes [1 is running in the mode and 0 otherwise].
x	Commitment status of the CSPP [1 is running and 0 otherwise].
γ	Auxiliary variable for the CVaR computation (Value-at-Risk).
Δ	Deviation amount between the generated and the scheduled power [MW].
Δ^+/Δ^-	Positive/Negative power deviation [MW].
η	Continuous positive variable for the CVaR computation.
ν^D/ν^I	Offered power of resources in the DA/ intraday market [MW].
ν^{FE}/ν^{SE}	Generated power via solar field/thermal energy storage in the CSPP [MW].
$\nu^{I,HPP,buy/sell}$	HPP's buying/ selling quantity in the intraday market [MW].
ν^{Sch}	The scheduled energy of resources [MW].
ϖ	Auxiliary variable in the ϵ-constraint method.
φ^D/φ^I	Electricity market price in the DA/ intraday market [€/MWh].

I. Introduction

In recent years, the power industry has experienced changes due to development from a regulated utility environment into a competitive and deregulated structure. However, the presence of new players, in both demand-side like demand response resources and supply-side such as clean energy resources, impose more complexity in controlling and handling of the power systems. From another standpoint, the environmentally-friendly and cost-effective natures of renewable resources are among those features that encourage their ever-increasing penetration. In contrast, the primary challenge facing the owners/operators of such renewable-driven systems is to cope with their intermittent nature.

Concentrating Solar Power Plant (CSPP) as an innovative supply-side player in the electricity market is a large-scale renewable energy resource. The CSPP is a zero-emission generating unit due to utilizing the thermal energy of the sun to run a steam turbine instead of utilizing fossil fuels, which results in financial savings [1]. However, benefiting from a thermal energy storage serves the CSPP to generate dispatchable energy, while other renewable energy resources such as wind and photovoltaic units produce intermittent electricity owing to the dependence of their output energy on instantaneous wind speed and solar irradiation [2]. Nevertheless, modeling the behavior of the CSPP in the presence of market price fluctuations and volatility in solar irradiation is considered as a significant challenge in electricity market studies.

The authors in [3] have proposed a scheduling scheme for a CSPP in which solar energy uncertainty has been modeled by various techniques such as stochastic and robust approaches, whereas the market price has been taken into account as a deterministic parameter. A robust optimization technique is utilized to model the solar irradiation uncertainty in [4] and [5], whereas the market price volatility is handled by a scenario-based stochastic framework. However, in [4], the CSPP merely participates in the Day-Ahead (DA) energy market, while its involvement in energy and ancillary service markets is addressed in [5]. In [6], a scenario-based stochastic structure, namely, downside risk, is utilized to reduce the risk-in-profit of a CSPP. In [7], the robust-based involvement of a CSPP coupled with a fossil-fuel power plant in the DA market has been presented.

On the other hand, the wind power as another clean energy resource has been widely scrutinized in the restructured electricity market to determine the optimal offering strategy under different uncertainties. A stochastic offering model for controlling the risk of wind power producer based on second-order stochastic dominance constraints has been suggested in [8]. In [9], the authors have concentrated on the offering strategy of wind units alongside a Demand Response Provider (DRP) tackling the uncertainties via a three-stage stochastic framework. The authors in [10] and [11] did two detailed studies on both profit maximization and emission minimization of a wind-thermal-battery storage system and a wind-thermal-photovoltaic power producer, respectively. Further, two comprehensive studies on the bidding strategy of wind-thermal-pumped storage systems by taking into account the CO_2 emission have been carried out in [12] and [13].

Moreover, Compressed Air Energy Storage (CAES), as a large-scale storage system, is a promising technology to facilitate the challenges and hurdles regarding the intermittent nature of renewable energy resources and market price uncertainty. In [14], a look-ahead model is provided to examine the optimal performance of the CAES in ancillary services, DA, and real-time energy markets to maximize its profit. In contrast, uncertain sources are neglected in their proposed framework [14]. A risk-constrained information gap decision theory-based bidding strategy for a CAES unit in the DA energy market is addressed in [15], while the uncertain parameter is the DA market price. The volatility of wind power in the self-scheduling problem has been managed via the CAES system in [16], whereas the Conditional Value-at-Risk (CVaR) is used to handle the financial risk of the three-stage stochastic model. In [17], an adaptive robust model is developed to derive the optimal self-scheduling of a wind-CAES producer under uncertainties related to forecasting inaccuracies of market price and wind power.

In terms of demand response resources and their influence on the offering strategy of various systems, several method-

ologies and architectures have been designed by the power system scholars. In [18], a stochastic structure for the optimal offering of a distributed energy resources aggregator in the attendance of demand response resources has been presented. In [19], the authors have concentrated on developing a robust-based bidding mechanism for industrial plants as a DRP. An incentive-based demand bidding model for a large consumer in the real-time market has been proposed in [20].

Accordingly, regarding the previous studies (Table I), the lack of presenting a comprehensive model incorporating flexible, green, and storage resources in the presence of different uncertainties for deriving their optimal behavior in the electricity markets is still a challenging issue in this area of research, which is addressed in this paper. Therefore, this paper aims to propose a new coordinated offering and bidding strategy for a Hybrid Power Producer (HPP), involving a CSPP, a wind farm, a CAES unit, and a DRP in DA and intraday electricity markets. The primary uncertain sources arising from involved market prices and renewable resources are modeled through a set of scenarios. Meanwhile, the entire decision-making process is divided into three distinct stages to address the offering and bidding problem fittingly. Moreover, the bi-objective optimization model of an apposite and efficient risk assessment technique, namely, CVaR, is incorporated into the suggested architecture to attain risk-involved strategies and improve the performance of previously applied CVaR-based frameworks to the offering and bidding strategy problems [9], [16]. The principal contributions of this paper compared to the reviewed literature in Table I can be summarized as follows:

1) Proposing a novel coordinated offering and bidding mechanism for an HPP containing a CSPP, a wind farm, a CAES unit, and a DRP. In the light of systems considered in the literature for the offering and bidding strategy problems, this is the first study that deals with the operation of an HPP having a CSPP, a CAES, a wind farm, and a DRP.
2) Examining the impact of the intraday market on the optimal participation of the CSPP. To the best of authors' knowledge, this paper is one of the first to investigate the influence of incorporating the intraday trading floor into the conventional DA offering models of a CSPP and appraise this influence in terms of both profitability and risk. According to Table I, none of the previous studies, whether a single CSPP or a CSPP paired with other resources, have performed such an analysis.
3) Establishing a bi-objective optimization model for CVaR-based offering and bidding strategy problems by means of ϵ-constraint and lexicographic methods and examining their superiority over the conventional weighted-sum technique. This approach and its key findings have not been reported in the literature of offering and bidding strategy problems up to our best knowledge.

The remainder of this paper is organized as follows. First, uncertainty characterization and decision-making framework are introduced in Section II. Then, the mathematical formulation of the proposed model is presented in Section III. The bi-objective CVaR-based trading strategy is described in Section IV. The simulation results are given in Section V, and eventually, the conclusions of this paper are highlighted in Section VI.

II. Uncertainty characterization and decision sequence

A. Uncertainty characterization

One of the challenges and concerns that researchers consistently encounter is how to address and incorporate uncertainties that are unavoidably present in most power system engineering issues. A variety of methods and approaches have been proposed to deal with this problem. In this paper, the primary uncertainties of the problem, namely, DA, intraday, and imbalance prices along with wind generation and produced thermal power by the solar field of the CSPP, are modeled by a scenario-based procedure to take advantage of the multi-stage stochastic programming structure. Towards this end, suitable probability density functions should be assigned for extracting the behavior of each uncertain parameter in every single time interval. In this context, the following distributions are utilized to analyze the statistical data of each uncertain parameter:

1) Electricity prices and the generated thermal power by the solar field of the CSPP: The normal distribution is used to address the uncertainty associated with electricity prices (φ^{price}) and the generated thermal power by the solar field of the CSPP (ESF) [6]. For instance, the normal distribution for electricity market prices is as follows:

$$f^{price}(\varphi^{price},\kappa^{price},\sigma^{price}) = \frac{1}{\sigma^{price}\sqrt{2\pi}} exp\left[-\frac{(\varphi^{price}-\kappa^{price})^2}{2(\sigma^{price})^2}\right] \quad (1)$$

where the κ^{price} and σ^{price} are the mean and the standard deviation of electricity prices, respectively.

2) Wind speed: Various distributions in the research literature, namely, the Weibull [21] and the Rayleigh [22], have been utilized in different circumstances to handle the uncertainty of wind speed (V). In the current paper, the wind speed is modeled via the Rayleigh distribution pursuant to the following equation [22]:

$$f^{wind}(V,c) = \frac{V}{c^2} exp\left[\frac{-V^2}{2c^2}\right] \quad (2)$$

where c is the scale factor of the Rayleigh distribution.

B. Decision sequence

Once the intended HPP aims to take part in the DA and intraday markets, it has to devise an appropriate decision-making framework based on the market structure and the uncertainty handling manner. In this paper, a three-stage stochastic programming scheme has been designed for modeling the optimal behavior of the considered HPP in electricity markets. The sequence of stages in the proposed three-stage decision-making framework is listed as follows:

1) There are two types of decisions in the first-stage decisions: *here-and-now* and *special here-and-now* decisions [23]. *Here-and-now* decisions are made by the HPP regarding the online/offline status of the CSPP and

TABLE I
COMPARISON BETWEEN THE ANALYZED WORKS AND THE PROPOSED FRAMEWORK IN THIS PAPER.

Ref.	System under study	Modeled markets			Modeling method	Risk model	CVaR modeling
		DA	Intraday	Balancing			
[3]	CSPP	✓	-	-	Robust/Stochastic MIP	Uncertainty budget	-
[4]	CSPP	✓	-	-	Robust+stochastic MIP	Uncertainty budget	-
[5]	CSPP	✓	-	✓	Robust MIP	Uncertainty budget	-
[6]	CSPP	✓	-	-	Stochastic MIP	Downside risk	-
[7]	CSPP+Fossil Fuel Power Plant	✓	-	-	Robust MIP	Uncertainty budget	-
[8]	Wind	✓	-	✓	Two-stage stochastic LP	SOSDCs	-
[9]	Wind+DRP	✓	✓	✓	Three-stage stochastic LP/MIP	CVaR	Weighting factor
[10]	Wind+Thermal+Battery	✓	-	✓	Two-stage stochastic MIP	-	-
[11]	Wind+Thermal+Photovoltaic	✓	-	✓	Stochastic MIP	-	-
[12]-[13]	Wind+Thermal+Pumped Storage	✓	-	✓	Stochastic MINLP	-	-
[14]	CAES	✓	-	✓	Deterministic MIP	-	-
[15]	CAES	✓	-	-	IGDT-based MINLP	R/O function	-
[16]	Wind+CAES	✓	✓	✓	Three-stage stochastic MIP	CVaR	Weighting factor
[17]	Wind+CAES	✓	-	✓	Adaptive Robust MIP	Uncertainty budget	-
[18]	Distributed Energy Resources	✓	-	-	Stochastic MIP	-	-
[19]	Industrial Plant	✓	-	-	Robust MIQP	Uncertainty budget	-
[20]	Large Industrial Consumer	✓	-	✓	Deterministic MIP	-	-
This Paper	CSPP+Wind+CAES+DRP	✓	✓	✓	Three-stage stochastic MIP	CVaR	ϵ-constraint

*N*ote: MIP-Mixed Integer Programming; LP-Linear Programming; SOSCDs-Second Order Stochastic Dominance Constraints; IGDT-Information Gap Decision Theory; MINLP-Mixed Integer Nonlinear Programming; R/O-Robustness/ Opportunity; MIQP-Mixed Integer Quadratic Programming

discharging/charging/simple-cycle mode of the CAES unit for the entire trading horizon, and accordingly, they do not depend on any scenario (e.g., x_t, u_t^{dis}) [23]. On the other hand, devising bidding and offering curves for the DA market are the *special here-and-now* decisions [23]. The word "*special*" is used due to the fact that these decisions are not single offering and bidding quantities, but they are curves and depend on the DA price realizations (e.g., $v_{t,\omega}^{D,CS}$, $v_{t,\omega}^{D,WF}$) [23]. In sum, the first-stage decisions are made prior to the realization of the stochastic processes, i.e., DA, intraday, and imbalance prices, along with wind generation and produced thermal power by the solar field.

2) Once the DA market prices are available to the HPP, the HPP decides on its selling and purchasing quantities in the intraday market. These are the second-stage decisions (*wait-and-see*1) that are made based upon the probable realization of intraday and imbalance prices, along with wind generation and produced thermal power by the solar field (e.g., $v_{t,\omega}^{I,CS}$, $v_{t,\omega}^{I,WF,sell}$) [24].
3) The third-stage decisions (*wait-and-see*2) appertain to the energy deviations imposed by the HPP in the last trading floor, namely, the balancing market. These decisions are made after the realization of all stochastic processes, including intraday and imbalance prices, along with wind generation and produced thermal power by the solar field ($\Delta_{t,\omega}^{+}$, $\Delta_{t,\omega}^{-}$) [24].

III. PROBLEM FORMULATION

In the coordinated trading strategy of all available resources, an optimization problem is established in which the optimal values of all decision variables will be obtained from the viewpoint of a single decision-making unit, namely, the HPP. The main aim is to maximize the expected profit of the whole system by running a single optimization problem. The CVaR-based trading strategy of the HPP comprises two objective functions, as given in the following subsections.

A. Objective function 1: Expected profit maximization

The objective function related to the HPP's expected profit is manifested in (3)-(4), where $Profit$ signifies the HPP's expected profit, and P_{ω}^{H} represents the HPP's profit in scenario ω. In (4), ξ_1 expresses the revenue of the HPP arising from the participation of the CSPP and the CAES unit in the DA market. ξ_2 represents the income resulting from the involvement of the wind farm and the DRP in the DA market, whereas ξ_3 stands for the DRP's incentive in the same market, and ξ_4 accounts for the cost of charging the CAES from the DA market. Note that, in this study, similar to [9], a fixed incentive rate plan is considered to model the DRP's incentive. It is important to remark that the independent system operator is in charge of determining the DRP's incentive for load reduction offers [9]. ξ_5 models the earnings associated with the CSPP and the CAES offering power quantities in the intraday market, while ξ_6 pertains to the expense of the CAES charging in the aforesaid market. It is worth mentioning that, analogous to [4], it has been assumed that the operating costs of the CSPP are negligible. The wind farm's revenue and cost in the intraday market are given by ξ_7. ξ_8 denotes the DRP's income in the intraday market, including both load reduction offer and the incentive payment. ξ_9 and ξ_{10} stand for the costs that originate from the operation of the CAES unit in both DA and intraday markets. The HPP's revenue concerning the price elasticity of the demand is shown in

ξ_{11}. Finally, ξ_{12} and ξ_{13} are related to the income and the cost of the system's positive and negative energy deviations in the balancing market, respectively. By focusing on the decision sequence expressed in the previous section, in (4), ξ_1-ξ_4, ξ_5-ξ_{11}, and ξ_{12}-ξ_{13} represent the expected profit of the HPP gained from the first-stage, second-stage, and third-stage of the suggested three-stage stochastic programming model, respectively.

$$Profit = \sum_{\omega=1}^{N_\Omega} \pi_\omega \times P_\omega^H \tag{3}$$

$$\begin{aligned} P_\omega^H = & \sum_{t=1}^{N_T} \underbrace{\varphi_{t,\omega}^D \nu_{t,\omega}^{D,CS} + \varphi_{t,\omega}^D \nu_{t,\omega}^{D,CA,dis} + \varphi_{t,\omega}^D \nu_{t,\omega}^{D,CA,s}}_{\xi_1} \\ & \underbrace{+\varphi_{t,\omega}^D \nu_{t,\omega}^{D,WF} + \varphi_{t,\omega}^D CL_{t,\omega}^D}_{\xi_2} \underbrace{+ \varphi^* CL_{t,\omega}^D}_{\xi_3} \underbrace{- \varphi_{t,\omega}^D \nu_{t,\omega}^{D,CA,ch}}_{\xi_4} \\ & \underbrace{+ \varphi_{t,\omega}^I \nu_{t,\omega}^{I,CS} + \varphi_{t,\omega}^I \nu_{t,\omega}^{I,CA,dis} + \varphi_{t,\omega}^I \nu_{t,\omega}^{I,CA,s}}_{\xi_5} \underbrace{- \varphi_{t,\omega}^I \nu_{t,\omega}^{I,CA,ch}}_{\xi_6} \\ & \underbrace{+ \varphi_{t,\omega}^I \nu_{t,\omega}^{I,WF,sell} - \varphi_{t,\omega}^I \nu_{t,\omega}^{I,WF,buy}}_{\xi_7} + \underbrace{\varphi_{t,\omega}^I CL_{t,\omega}^I + \varphi^* CL_{t,\omega}^I}_{\xi_8} \\ & \underbrace{- \nu_{t,\omega}^{Sch,CA,dis} \left(Htr^{dis} \times GP + OM^{exp} \right) - \nu_{t,\omega}^{Sch,CA,ch} OM^{co}}_{\xi_9} \\ & \underbrace{- \nu_{t,\omega}^{Sch,CA,s} \left(Htr^{s} \times GP + OM^{exp} + OM^{co} \right)}_{\xi_{10}} \\ & \underbrace{+ \frac{1}{2\Upsilon L_{0,t}} \sum_{b=1}^{N_B} S_b CL_{b,t,\omega}^{Sch\_b}}_{\xi_{11}} + \underbrace{\left(\varphi_{t,\omega}^D r_{t,\omega}^+ \Delta_{t,\omega}^+ \right)}_{\xi_{12}} - \underbrace{\left(\varphi_{t,\omega}^D r_{t,\omega}^- \Delta_{t,\omega}^- \right)}_{\xi_{13}} \end{aligned} \tag{4}$$

B. Objective function 2: CVaR maximization

The second objective function, i.e., $CVaR$, strives to manage the risk in the trading strategy process, which is formulated as follows [9], [16]:

$$CVaR = \gamma - \frac{1}{1-\alpha} \sum_{\omega=1}^{N_\Omega} \pi_\omega \eta_\omega \tag{5}$$

The constraints of both objective functions are presented in the following.

1) Modeling of the CSPP: Equation (6) represents the offered power from the CSPP in both DA and intraday markets, which originates from both solar field and thermal energy storage facility [4]. The total scheduled power of the CSPP, solar field, and thermal energy storage are calculated according to equation (7).

$$\begin{bmatrix} \nu_{t,\omega}^{D,CS} \\ \nu_{t,\omega}^{I,CS} \end{bmatrix} = \begin{bmatrix} \nu_{t,\omega}^{D,FE} \\ \nu_{t,\omega}^{I,FE} \end{bmatrix} + \begin{bmatrix} \nu_{t,\omega}^{D,SE} \\ \nu_{t,\omega}^{I,SE} \end{bmatrix} \quad \forall t, \forall \omega \tag{6}$$

$$\begin{bmatrix} \nu_{t,\omega}^{Sch,CS} \\ \nu_{t,\omega}^{Sch,FE} \\ \nu_{t,\omega}^{Sch,SE} \end{bmatrix} = \begin{bmatrix} \nu_{t,\omega}^{D,CS} \\ \nu_{t,\omega}^{D,FE} \\ \nu_{t,\omega}^{D,SE} \end{bmatrix} + \begin{bmatrix} \nu_{t,\omega}^{I,CS} \\ \nu_{t,\omega}^{I,FE} \\ \nu_{t,\omega}^{I,SE} \end{bmatrix} \quad \forall t, \forall \omega \tag{7}$$

Constraint (8) limits the upper and lower bounds of the CSPP's DA offer and the total CSPP's scheduled power within the CSPP's nominal capacity. The total scheduled electric power of the solar field and the thermal energy storage are computed using (9) and (10), respectively [4].

$$\begin{bmatrix} 0 \\ 0 \end{bmatrix} \leq \begin{bmatrix} \nu_{t,\omega}^{D,CS} \\ \nu_{t,\omega}^{Sch,CS} \end{bmatrix} \leq \begin{bmatrix} CP^{CS} \\ CP^{CS} \end{bmatrix} \quad \forall t, \forall \omega \tag{8}$$

$$\nu_{t,\omega}^{Sch,FE} = \lambda_1 Q_{t,\omega}^{FE} \quad \forall t, \forall \omega \tag{9}$$

$$\nu_{t,\omega}^{Sch,SE} = \lambda_3 Q_{t,\omega}^{SE} \quad \forall t, \forall \omega \tag{10}$$

Restrictions (11)-(14) define the ramp down and ramp up limitations of the thermal energy storage [4]. Constraint (15) restricts the upper bound of the total utilized thermal power of the solar field within the thermal power realization in the solar field on the basis of the solar power [4].

$$\nu_{t,\omega}^{Sch,SE} - \nu_{t+1,\omega}^{Sch,SE} \leq RD^{dis} \quad \forall t = 0, \ldots, N_T - 1, \forall \omega \tag{11}$$

$$\nu_{t+1,\omega}^{Sch,SE} - \nu_{t,\omega}^{Sch,SE} \leq RU^{dis} \quad \forall t = 0, \ldots, N_T - 1, \forall \omega \tag{12}$$

$$\lambda_2 \left(Q_{t+1,\omega}^{FS} - Q_{t,\omega}^{FS} \right) \leq RU^{ch} \quad \forall t = 0, \ldots, N_T - 1, \forall \omega \tag{13}$$

$$\lambda_2 \left(Q_{t,\omega}^{FS} - Q_{t+1,\omega}^{FS} \right) \leq RD^{ch} \quad \forall t = 0, \ldots, N_T - 1, \forall \omega \tag{14}$$

$$Q_{t,\omega}^{FE} + Q_{t,\omega}^{FS} \leq ESF_{t,\omega} \quad \forall t, \forall \omega \tag{15}$$

Constraint (16) ensures that the total thermal power employed for electric power generation does not exceed its allowable ranges [4]. Equations (17) and (18) computes the stored energy in the thermal energy storage for the first and remaining periods of the trading horizon, while constraint (19) keeps the stored energy in the thermal energy storage within the permissible range [4]. Other CSPP's restrictions, including minimum off/on time, are modeled similar to the approach proposed in [10]. Constraint (20) states that the stored energy in the thermal energy storage for the first and the last periods of the trading horizon must be equal.

$$Q^{E,Min} x_t \leq Q_{t,\omega}^{FE} + Q_{t,\omega}^{SE} \leq Q^{E,Max} x_t \quad \forall t, \forall \omega \tag{16}$$

$$Q_{t,\omega}^{S} = Q_0 + \lambda_2 Q_{t,\omega}^{FS} - Q_{t,\omega}^{SE} \quad \forall t = 1, \forall \omega \tag{17}$$

$$Q_{t,\omega}^{S} = Q_{t-1,\omega}^{S} + \lambda_2 Q_{t,\omega}^{FS} - Q_{t,\omega}^{SE} \quad \forall t \geq 2, \forall \omega \tag{18}$$

$$Q^{S,Min} \leq Q_{t,\omega}^{S} \leq Q^{S,Max} \quad \forall t, \forall \omega \tag{19}$$

$$Q_{t=24,\omega}^{S} = Q_0 \quad \forall \omega \tag{20}$$

2) Constraints of the CAES: Equation (21) defines the scheduled power of the CAES unit in different operating modes, whereas constraints (22) and (23) impose the limitations of the DA offering quantities and the scheduled energy of the CAES unit [16]. Constraint (24) ensures that the CAES unit only operates in one operating mode for any scheduling period [16]. In (22)-(24), u_t^s represents the simple-cycle mode of the CAES unit. It should be noted that the simple-cycle is an operational mode in which the CAES unit runs as a gas turbine [16].

$$\begin{bmatrix} \nu_{t,\omega}^{Sch,CA,dis} \\ \nu_{t,\omega}^{Sch,CA,s} \\ \nu_{t,\omega}^{Sch,CA,ch} \end{bmatrix} = \begin{bmatrix} \nu_{t,\omega}^{D,CA,dis} \\ \nu_{t,\omega}^{D,CA,s} \\ \nu_{t,\omega}^{D,CA,ch} \end{bmatrix} + \begin{bmatrix} \nu_{t,\omega}^{I,CA,dis} \\ \nu_{t,\omega}^{I,CA,s} \\ \nu_{t,\omega}^{I,CA,ch} \end{bmatrix} \forall t, \forall \omega \tag{21}$$

$$\begin{bmatrix} 0 \\ 0 \\ 0 \end{bmatrix} \leq \begin{bmatrix} \nu_{t,\omega}^{D,CA,dis} \\ \nu_{t,\omega}^{D,CA,s} \\ \nu_{t,\omega}^{D,CA,ch} \end{bmatrix} \leq \begin{bmatrix} CP^{exp} u_t^{dis} \\ CP^{exp} u_t^{s} \\ CP^{co} u_t^{ch} \end{bmatrix} \quad \forall t, \forall \omega \tag{22}$$

$$\begin{bmatrix} 0 \\ 0 \\ 0 \end{bmatrix} \leq \begin{bmatrix} \nu_{t,\omega}^{Sch,CA,dis} \\ \nu_{t,\omega}^{Sch,CA,s} \\ \nu_{t,\omega}^{Sch,CA,ch} \end{bmatrix} \leq \begin{bmatrix} CP^{exp} u_t^{dis} \\ CP^{exp} u_t^{s} \\ CP^{co} u_t^{ch} \end{bmatrix} \quad \forall t, \forall \omega \tag{23}$$

$$u_t^{dis} + u_t^{s} + u_t^{ch} \leq 1 \quad \forall t \tag{24}$$

The storage energy level in each time interval is expressed by equation (25)-(26), while limitation (27) retains the storage energy level within the available capacity [16]. Equation (28) enforces the equality constraint of the energy in the CAES storage for the first and the last periods of the scheduling horizon.

$$EC_{t,\omega}^{CA} = EC_0^{CA} + ER \times \left(\nu_{t,\omega}^{Sch,CA,dis} - \nu_{t,\omega}^{Sch,CA,ch} \right) \quad \forall t = 1, \forall \omega \tag{25}$$

$$EC_{t,\omega}^{CA} = EC_{t-1,\omega}^{CA} + ER \times \left(\nu_{t,\omega}^{Sch,CA,dis} - \nu_{t,\omega}^{Sch,CA,ch} \right) \quad \forall t \geq 2, \forall \omega \tag{26}$$

$$0 \leq EC_{t,\omega}^{CA} \leq EC^{Max} \quad \forall t, \forall \omega \tag{27}$$

$$EC_{t=24,\omega}^{CA} = EC_0^{CA} \quad \forall \omega \tag{28}$$

3) Constraints of the DRP and Wind Farm: Equation (29) expresses the scheduled power of the wind farm, which is equal to the sum of selling values in the DA and intraday market minus the purchasing energy from the intraday market [9]. Constraint (30) restricts the upper and lower bounds of the DA offering values of the wind farm [10]. In (31)-(32), the scheduled DRP's load reduction offer is denoted [9], while in (33), the upper bounds of the DA and the scheduled load reduction offers are enforced [9]. Restriction (34) enforces the limit of the scheduled load reduction offer in the entire trading horizon [9].

$$\nu_{t,\omega}^{Sch,WF} = \nu_{t,\omega}^{D,WF} + \nu_{t,\omega}^{I,WF,sell} - \nu_{t,\omega}^{I,WF,buy}, \quad \forall t, \forall \omega \tag{29}$$

$$0 \leq \nu_{t,\omega}^{D,WF} \leq CP^{WF} \quad \forall t, \forall \omega \tag{30}$$

$$CL_{t,\omega}^{Sch} = CL_{t,\omega}^{D} + CL_{t,\omega}^{I} \quad \forall t, \forall \omega \tag{31}$$

$$CL_{t,\omega}^{Sch} = \sum_{b=1}^{N_B} CL_{b,t,\omega}^{Sch\_b} \quad \forall t, \forall \omega \tag{32}$$

$$\begin{bmatrix} 0 \\ 0 \end{bmatrix} \leq \begin{bmatrix} CL_{t,\omega}^{D} \\ CL_{t,\omega}^{Sch} \end{bmatrix} \leq \delta \begin{bmatrix} L_{0,t} \\ L_{0,t} \end{bmatrix} \quad \forall t, \forall \omega \tag{33}$$

$$\sum_{t=1}^{N_T} CL_{t,\omega}^{Sch} \leq \mu \sum_{t=1}^{N_T} L_{0,t} \quad \forall t, \forall \omega \tag{34}$$

4) Coordinated offering and bidding constraints: The total scheduled power of the HPP in both intraday and DA markets is equal to the sum of the scheduled power of all available resources, as expressed in (35). In the coordinated trading strategy, the total acceptable volume of selling and buying energies in the intraday market is computed in (36) and (37), respectively, whereas constraints (38) and (39) are fulfilled to enforce these requirements. To meet the requirement of the HPP's scheduled energy, constraint (40) keeps this variable within the acceptable range. The total HPP's imbalances are denoted in (41), while constraints (42) and (43) represent that the HPP's positive and negative imbalances are restricted within the permissible values. It has to be noted that positive energy deviation, i.e., positive imbalance, occurs when the scheduled energy of the HPP is less than the total actual power of the HPP. Similarly, negative energy deviation refers to the situations that the HPP's scheduled energy is greater than the real output power of the HPP.

$$\nu_{t,\omega}^{Sch,HPP} = \nu_{t,\omega}^{Sch,CS} + \nu_{t,\omega}^{Sch,WF} + \nu_{t,\omega}^{Sch,CA,dis} + \nu_{t,\omega}^{Sch,CA,s} + CL_{t,\omega}^{Sch} \quad \forall t, \forall \omega \tag{35}$$

$$CP^{I,HPP,sell} = \Gamma \times \left(\mathrm{CP^{CS}} + \mathrm{CP^{exp}} + \mathrm{CP^{WF}} + \delta \mathrm{L_{0,t}} \right) \tag{36}$$

$$CP^{I,HPP,buy} = \Gamma \times \left(CP^{co} + CP^{WF} \right) \tag{37}$$

$$0 \leq \nu_{t,\omega}^{I,CS} + \nu_{t,\omega}^{I,CA,dis} + \nu_{t,\omega}^{I,CA,s} + \nu_{t,\omega}^{I,WF,sell} + CL_{t,\omega}^{I} \leq CP^{I,HPP,sell} \quad \forall t, \forall \omega \tag{38}$$

$$0 \leq \nu_{t,\omega}^{I,CA,ch} + \nu_{t,\omega}^{I,WF,buy} \leq CP^{I,HPP,buy} \quad \forall t, \forall \omega \tag{39}$$

$$0 \leq \nu_{t,\omega}^{Sch,HPP} \leq CP^{CS} x_t + CP^{exp} u_t^{dis} + CP^{exp} u_t^{s} + CP^{WF} + \delta L_{0,t} \quad \forall t, \forall \omega \tag{40}$$

$$\Delta_{t,\omega} = \Delta_{t,\omega}^{+} - \Delta_{t,\omega}^{-} = PW_{t,\omega} - \nu_{t,\omega}^{Sch,WF} \quad \forall t, \forall \omega \tag{41}$$

$$0 \leq \Delta_{t,\omega}^{-} \leq CP^{CS} x_t + CP^{exp} u_t^{dis} + CP^{exp} u_t^{s} + CP^{WF} + \delta L_{0,t} \quad \forall t, \forall \omega \tag{42}$$

$$0 \leq \Delta_{t,\omega}^{+} \leq PW_{t,\omega} + \nu_{t,\omega}^{Sch,CS} + \nu_{t,\omega}^{Sch,CA,dis} + \nu_{t,\omega}^{Sch,CA,s} + CL_{t,\omega}^{Sch} \quad \forall t, \forall \omega \tag{43}$$

Restriction (44) ensures that the offering curves of the CSPP, CAES, and wind farm in the DA market must be non-decreasing, while constraint (45) guarantees the decreasing state of bidding curves. In this regard, the non-anticipativity rule of the DA and intraday offering and bidding quantities is enforced by constraints (46) and (47), respectively. Finally, the description of constraints (48) and (49) corresponds to the given descriptive statements of restrictions (44) and (46)-(47), respectively.

$$\nu_{t,\omega}^{D,\psi_1} \leq \nu_{t,\widetilde{\omega}}^{D,\psi_1}, \quad \forall \omega, \widetilde{\omega} : [\varphi_{t,\omega}^{D} \leq \varphi_{t,\widetilde{\omega}}^{D}], \quad \forall t \quad \& \quad \psi_1 = [CS,WF,(CA,dis),(CA,s)] \tag{44}$$

$$\nu_{t,\omega}^{D,CA,ch} \leq \nu_{t,\widetilde{\omega}}^{D,CA,ch}, \quad \forall \omega, \widetilde{\omega} : [\varphi_{t,\omega}^{D} \geq \varphi_{t,\widetilde{\omega}}^{D}], \quad \forall t \tag{45}$$

$$\nu_{t,\omega}^{D,\psi_2} = \nu_{t,\widetilde{\omega}}^{D,\psi_2}, \quad \forall \omega, \widetilde{\omega} : [\varphi_{t,\omega}^{D} = \varphi_{t,\widetilde{\omega}}^{D}], \quad \forall t \quad \& \quad \psi_2 = [CS,WF,(CA,dis),(CA,s),(CA,ch)] \tag{46}$$

$$\nu_{t,\omega}^{I,\psi_3} = \nu_{t,\widetilde{\omega}}^{I,\psi_3}, \quad \forall \omega, \widetilde{\omega} : [\varphi_{t,\omega}^{D} = \varphi_{t,\widetilde{\omega}}^{D}], \quad \forall t \quad \& \quad \psi_3 = [CS,(WF,sell),(WF,buy),(CA,dis),(CA,s),(CA,ch)] \tag{47}$$

$$CL_{t,\omega}^{D} \leq CL_{t,\widetilde{\omega}}^{D}, \quad \forall \omega, \widetilde{\omega} : [\varphi_{t,\omega}^{D} \leq \varphi_{t,\widetilde{\omega}}^{D}], \quad \forall t \tag{48}$$

$$\begin{bmatrix} CL_{t,\omega}^{D} \\ CL_{t,\omega}^{I} \end{bmatrix} = \begin{bmatrix} CL_{t,\widetilde{\omega}}^{D} \\ CL_{t,\widetilde{\omega}}^{I} \end{bmatrix} \quad \forall \omega, \widetilde{\omega} : [\varphi_{t,\omega}^{D} = \varphi_{t,\widetilde{\omega}}^{D}], \quad \forall t \tag{49}$$

C. CVaR constraints

Considering the CVaR risk measuring index, constraints (50) and (51) pertain to the CVaR calculation. In constraint (50), P_{ω}^{H} stands for the HPP's profit in scenario ω, and η_{ω} is an ancillary variable representing the difference of HPP's profit in scenario ω and the value-at-risk (γ). Constraint (51) enforces that this difference must be non-negative. In other words, the value of η_{ω} is set to zero for a specific scenario in which the HPP's profit becomes greater than the value-at-risk (γ). Overall, objective function (5) along with constraints (50) and (51) computes the CVaR for the HPP's profit distribution [9], [16].

$$\gamma - P_{\omega}^{H} \leq \eta_{\omega} \quad \forall \omega \tag{50}$$

$$\eta_{\omega} \geq 0 \quad \forall \omega \tag{51}$$

IV. Solution Approach

As previously outlined, the optimization problems under CVaR risk measure are bi-objective optimization problems, which are mainly solved using weighted-sum approach to attain Pareto solutions ([9], [16], and [23]-[25]). By focusing on the weighted-sum technique, the CVaR-constrained optimal trading strategy is formulated as follows:

$$\begin{aligned} &\text{Max} \quad (1-\beta) \times Profit + (\beta) \times CVaR \\ &\text{Subject to} : (3)-(51), \quad 0 \leq \beta \leq 1 \end{aligned} \tag{52}$$

Notwithstanding the simple implementation of the weighted-sum method, this method suffers from: 1) the complexity and the hardness of specifying proper weighting factors for the objective functions when sufficient information is not available to the decision-maker; 2) generating unevenly spaced Pareto solutions; 3) not being able to impose the preferences of the decision-maker for producing Pareto solutions; 4) imposing further computational cost for suitable scaling of the objective functions [26]. More specifically, as it has been argued in [10], a slight change in the weighting factor may lead to considerable variation in the value of objective functions. To overcome several drawbacks noted for the weighted-sum approach [26], the improved version of the ϵ-constraint method, namely, augmented ϵ-constraint technique, alongside lexicographic optimization framework, is utilized [10]. It is worthwhile to note that the improved version of the ϵ-constraint method eliminates all the above-mentioned weaknesses of the weighted sum technique [26]. The lexicographic method facilitates obtaining efficient solutions to build the pay-off table, PT, and as a result, to determine the range of each objective function. The pay-off table is shown in (53), whereas each element of PT is obtained through the lexicographic technique (54)-(57).

$$PT = \begin{bmatrix} PT_{1,1} & PT_{1,2} \\ PT_{2,1} & PT_{2,2} \end{bmatrix} \tag{53}$$

$$PT_{1,1} = Profit^{\star} : \begin{pmatrix} \text{Max} \quad Profit \\ \text{Subject to} : (3)-(51) \end{pmatrix} \tag{54}$$

$$PT_{2,2} = CVaR^{\star} : \begin{pmatrix} \text{Max} \quad CVaR \\ \text{Subject to} : (3)-(51) \end{pmatrix} \tag{55}$$

$$PT_{1,2} = CVaR^{\circ} : \begin{pmatrix} \text{Max} \quad CVaR \\ \text{Subject to} : (3)-(51) \ \& \ Profit = PT_{1,1} \end{pmatrix} \tag{56}$$

$$PT_{2,1} = Profit^{\circ} : \begin{pmatrix} \text{Max} \quad Profit \\ \text{Subject to} : (3)-(51) \ \& \ CVaR = PT_{2,2} \end{pmatrix} \tag{57}$$

where $Profit^{\star}$ and $CVaR^{\star}$ are the *Utopia* points (best values), and $Profit^{\circ}$ and $CVaR^{\circ}$ are the *Pseudo Nadir* points (worst values) of both objective functions. By having the pay-off table, the CVaR-based trading strategy using the improved version of the ϵ-constraint method is formed as below:

$$\begin{aligned} &\text{Max} \quad Profit - \frac{\varpi}{(PT_{2,2} - PT_{1,2})} \\ &\text{Subject to} : CVaR - \varpi = \varrho_j \\ &\qquad \varrho_j = PT_{1,2} + \left(\frac{PT_{2,2} - PT_{1,2}}{h} \right) \times j, \quad j = 0, 1, ..., h \\ &\qquad (3)-(51) \quad \& \quad \varpi \geq 0 \end{aligned} \tag{58}$$

where ϖ is an auxiliary variable, j represents the grid point number, and $(PT_{2,2} - PT_{1,2})$ stands for the range of the CVaR. In order to attain various Pareto solutions to construct the Pareto frontier, $(h+1)$ grid points are considered, and accordingly, the optimization problem divides into $(h+1)$ sub-problems that must be solved. Further details on the lexicographic method and improved version of the ϵ-constraint technique can be found in [10].

V. Numerical results

The considered HPP is composed of a CSPP, a CAES unit, a wind farm, and a DRP. The nominal capacity of the wind farm is 40 MW. The characteristics of the CAES unit and the confidence level used for the CVaR calculation have been reported in Table II. According to this table, the maximum charging and discharging powers of the CAES unit are 60 MW and 100 MW, respectively, while the CAES storage size is considered equal to 20 hours of its full discharging capacity. The data on the DRP and the CSPP are presented in Table III. The load profile of the DRP prior to applying the demand response program for its optimal behavior in the target markets is shown in Fig. 1 [29].

As stated in section II, the uncertainties that originate from renewable resources and electricity markets are characterized via a set of scenarios. It is worthwhile to mention that the mean values of thermal generation by the solar field have been adopted from [4], while ten percent of the mean values have been assumed as the standard deviations of each specific hour.

A six-month examination on the parameters of the Spanish electricity market [31] has been fulfilled to get the parameters of the normal distribution, i.e., mean and standard deviation. Likewise, by benefiting from the wind speed data of [32] for the identical time interval, twenty-four Rayleigh distributions corresponding to each scheduling period are obtained. Given the probability density functions of each uncertain parameter,

TABLE II
TECHNICAL SPECIFICATIONS OF THE CAES SYSTEM AND THE CVAR CONFIDENCE LEVEL.

Parameter	Value	Ref.	Parameter	Value	Ref.
CP^{exp} [MW]	100	[27]	GP [€/MBtu]	4.6	[28]
CP^{co}[MW]	60	[27]	ER [%]	95	[16]
EC^{Max} [MWh]	2000	[15]	$OM^{exp/co}$ [€/MWh]	3	[28]
Htr^{dis} [MBtu/MWh]	4.07	[28]	Htr^{s} [MBtu/MWh]	10.83	[28]
EC_0^{CA} [MWh]	0	[15]	α	0.95	[9]

TABLE III
INFORMATION ON THE CSPP, THE DRP, AND OTHER INPUT PARAMETERS.

Parameter	Value	Ref.	Parameter	Value	Ref.
Υ	-0.3	[29]	μ	0.04	[29]
φ^*	0.3	[29]	δ	0.2	[29]
Γ	0.3	[29]	Q_0 [MWh]	350	[4]
CSP^{CS} [MW]	50	[4]	RU^{ch}[MW/h]	80	[4]
$Q^{E,Min}$ [MW]	50	[4]	RU^{dis}[MW/h]	80	[4]
$Q^{E,Max}$ [MW]	125	[4]	RD^{ch} [MW/h]	35	[4]
$Q^{S,Min}$ [MWh]	45	[4]	RD^{dis} [MW/h]	35	[4]
$Q^{S,Max}$ [MWh]	700	[4]	λ_1 [%]	40	[4]
λ_2 [%]	80	[4]	λ_3 [%]	35	[4]

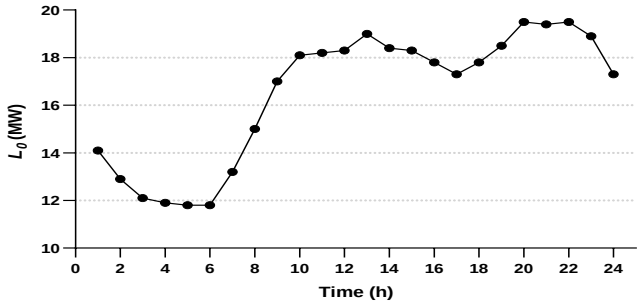

Fig. 1. DRP's load curve before participating in the DA and intraday markets.

a large number of scenarios (in this paper, 5000 scenarios) are generated to model the behavior of random parameters. Subsequently, to keep tractability, SCENRED2 [30] is implemented to reduce the number of scenarios. To this end, the number of scenarios related to wind and thermal production of the CSPP, as well as DA market scenarios, is reduced to ten scenarios. In contrast, the generated intraday and balancing market scenarios are lessened to six scenarios. Regarding the proposed three-stage architecture, the scenario tree possesses 3600 scenarios with the 10×6×6×10 construction. It is worth mentioning that the procedure of scenario generation for imbalance market prices is similar to the technique suggested in [9] and [16].

To demonstrate the usefulness and effectiveness of the proposed coordinated offering and bidding framework, two different case studies have been created as follows:

- Case 1: The first case study concerns with the disjoint involvement of the considered resources in the target markets (the disjoint configuration). In this case study, all elements of the HPP participate in the intended markets individually.
- Case 2: The second case study pertains to the coordinated offering and bidding of all existing resources (joint configuration). In this case study, all available resources participate in the DA and intraday markets from the standpoint of a unit HPP.

A. Impact of different configurations on the expected profit and risk of the system

The results of the expected profit and CVaR in both configurations for different risk-averse levels employing both weighted-sum and ϵ-constraint methods have been presented in Fig. 2. To derive the efficient frontier using weighted-sum approach, eleven equally spaced points for β, β= [0, 0.1, 0.2, 0.3, …, 0.9, 1], are utilized. Likewise, after obtaining the pay-off table by solving optimization problems (54)-(57) (lexicographic approach), eleven grid points j= [0, 1, 2, 3, …, 9, 10] are exploited to find the efficient frontier through the ϵ-constraint method. According to the obtained efficient frontiers and results presented in Tables IV and V, it can be concluded that the ϵ-constraint method has the following advantages over the weighted-sum approach: 1) it obtains equally spaced Pareto solutions in terms of CVaR, whereas the weighted-sum cannot; 2) for the risk-neutral case, it derives a solution with a lower level of risk in comparison with the weighted-sum method, while the obtained expected profit for both methods is equivalent; and 3) for the case with the highest degree of risk-aversion, it draws a solution with a greater value of the expected profit compared to the weighted-sum method, while the attained CVaR for both techniques is equal.

Furthermore, a comparison between the computational size of the elaborated Mixed-Integer Programming (MIP) problem for Case 2 under two different solution approaches, i.e., weighted-sum and ϵ-constraint, has been given in Table VI. Both case studies are optimized with the CPLEX solver in General Algebraic Modeling System (GAMS) on a laptop computer with 4 GB of RAM and a Core i5 processor. It has to be noted that the gap setting in the CPLEX solver has been set to zero to ensure reaching the global optimum solution. According to Table VI, it is clear that there is no significant difference between the average sub-problem solution time of both solution approaches. The higher computational cost of the proposed approach compared to the weighted-sum technique appertains to the lexicographic method.

Regardless of the solution approach (weighted-sum or ϵ-constraint), it can be seen from Fig. 2 that the joint configuration is capable of improving both expected profit and CVaR for similar values of β and j. According to these results, the joint configuration not only leads to profitability, but also lessens the total risk. To demonstrate the expected profit and CVaR gains in the joint configuration for all Pareto solutions (P1-P11), Fig. 3 has been provided. It is noteworthy to say that P1 and P11 in Fig. 3 represent the risk-neutral and the highest degree of risk-aversion states, respectively. From Fig. 3, it is seen that

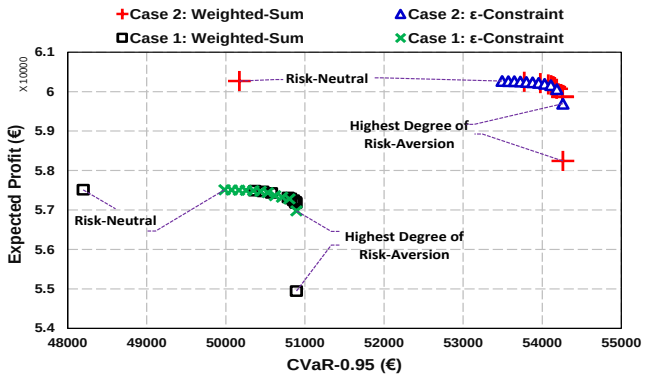

Fig. 2. Efficient frontier in joint and disjoint configurations employing weighted-sum and ϵ-constraint techniques.

TABLE IV
COMPARISON BETWEEN RESULTS OBTAINED THROUGH WEIGHTED-SUM AND ϵ-CONSTRAINT TECHNIQUES IN CASE 1.

Approach	Risk-Neutral		Highest Degree of Risk-Aversion	
	Expected Profit (€)	CVaR-0.95 (€)	Expected Profit (€)	CVaR-0.95 (€)
Weighted-Sum	57,511.02	48,195.97	54,945.82	50,892.29
ϵ-Constraint	57,511.02	49,982.70	56,977.49	50,892.29

TABLE V
COMPARISON BETWEEN RESULTS OBTAINED THROUGH WEIGHTED-SUM AND ϵ-CONSTRAINT TECHNIQUES IN CASE 2.

Approach	Risk-Neutral		Highest Degree of Risk-Aversion	
	Expected Profit (€)	CVaR-0.95 (€)	Expected Profit (€)	CVaR-0.95 (€)
Weighted-Sum	60,268.15	50,171.30	58,242.09	54,260.08
ϵ-Constraint	60,268.15	53,493.09	59,693.69	54,260.08

for Pareto solutions P1-P10, the joint configuration achieves the almost equivalent level of expected profit gain with an amount of more than 4%, regardless of the solution approach. Only in P11 (highest degree of risk-aversion), the weighted-sum technique obtains a higher expected profit gain compared to the ϵ-constraint method, whereas the final earned expected profit through the ϵ-constraint approach is greater than the weighted-sum method. In contrast, a considerable discrepancy between the CVaR gains of the weighted-sum and ϵ-constraint methods in the risk-neutral state (P1) is felt, while for other Pareto solutions (P2-P11), an approximately equal level of the CVaR gain for both solution approaches is reached. Overall, the joint configuration not only guarantee the profitability of the proposed offering and bidding architecture, but also is able to decrease the associated risk.

Based on the foregoing, from now on, all presented results appertain to the ϵ-constraint method owing to its better performance compared to the weighted-sum technique. Fig. 4 and Fig. 5 show the hourly expected profit of each HPP's element in risk-neutral and highest degree of risk-aversion strategies, respectively. As shown in Fig. 4 and Fig. 5, in both strategies,

TABLE VI
COMPUTATIONAL SIZE OF THE CONSIDERED PROBLEM IN CASE 2.

Number of binary variables (weighted-sum and ϵ-constraint)	144
Number of continuous variables using weighted-sum	26,008
Number of continuous variables using ϵ-constraint	26,009
Number of equations using weighted-sum	39,585
Number of equations using ϵ-constraint	39,586
Solution time of all Pareto points using Weighted-sum (sec)	105
Average sub-problem solution time using Weighted-sum (sec)	9.54
Solution time of pay-off matrix using lexicographic method (sec)	353
Solution time of all Pareto points using ϵ-constraint (sec)	124
Average sub-problem solution time using ϵ-constraint (sec)	11.27

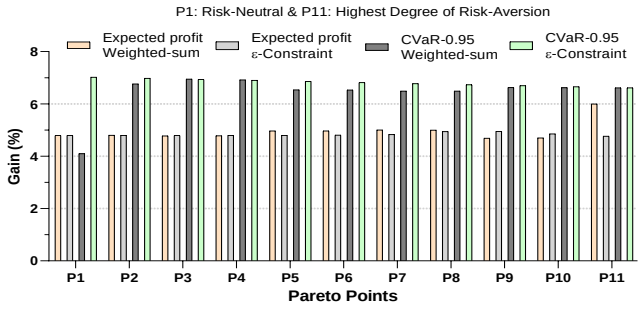

Fig. 3. The gain of expected profit and CVaR in the joint configuration employing weighted-sum and ϵ-constraint techniques.

joint and disjoint configurations impose a greater impact on the hourly expected profit of the wind farm and the CSPP. Similarly, the CAES unit and the DRP undergo the lowest change. This issue is also true for the share of each resource from the total expected profit, which has been shown in Fig. 6. From this figure, it is observed that much of the HPP's profit come from the wind farm and the CSPP. Another critical point that can be deduced from Fig. 4 is that the CAES unit merely operates in the simple-cycle model in the risk-neutral strategy as it does not have any negative value in Fig. 4. In contrast, in the strategy with the highest degree of risk-aversion (Fig. 5), the CAES unit experiences all operating modes, i.e., charging, discharging, and simple-cycle.

B. Impact of the intraday market and the joint configuration on the CSPP

This study has been defined to assess the consequence of the joint configuration and embracing the intraday market from the viewpoint of the CSPP. In the first part of this analysis, the impact of the aforesaid factors on the CSPP's expected profit and CVaR is investigated. To this end, a further study, focusing on the DA offering of the CSPP in the disjoint configuration, is accomplished. Fig. 7 compares the results of the expected profit and CVaR in various CSPP's operational strategies: 1) uncoordinated operation of the CSPP in the DA market; 2) uncoordinated operation of the CSPP in joint DA and intraday markets; and 3) coordinated operation of the CSPP with other available resources in both DA and intraday markets (Case 2). According to this figure, it can be concluded that incorporating the intraday market into the proposed offering structure leads

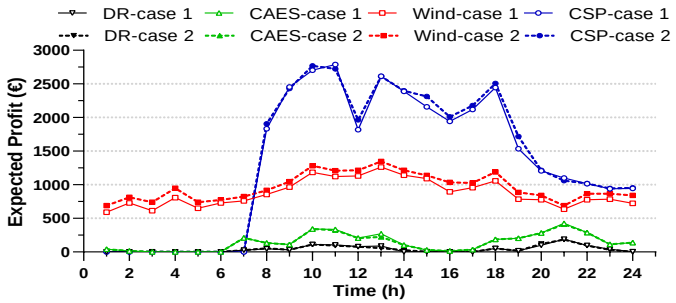

Fig. 4. Hourly expected profit of each resource for joint and disjoint configurations in the risk-neutral state using ϵ-constraint technique.

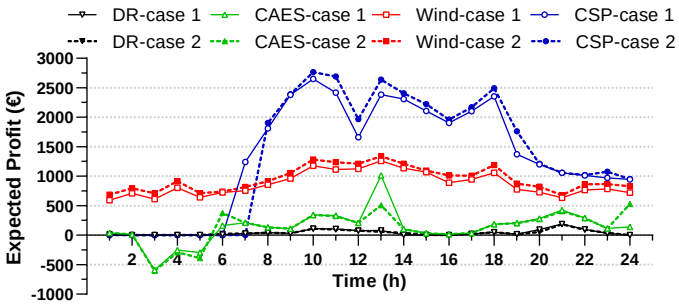

Fig. 5. Hourly expected profit of each resource for joint and disjoint configurations in the state with the highest degree of risk-aversion using ϵ-constraint technique.

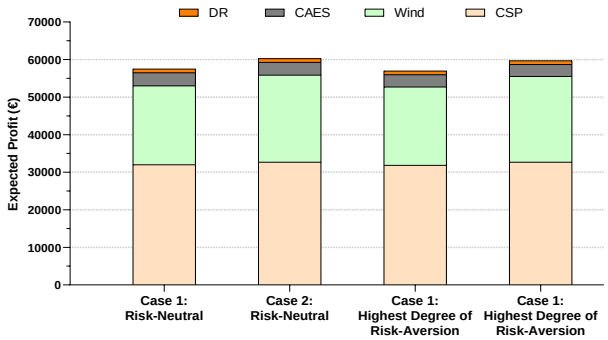

Fig. 6. Share of each resource from the total expected profit in different operational strategies.

to both profitability and risk-mitigating of the CSPP. Another noteworthy point that can be deduced from this figure is that, in addition to including the intraday market, the joint configuration also results in the improvement of the CSPP's operation in terms of the expected profit.

The comparison between the total DA and intraday offers of the CSPP, along with the total CSPP's scheduled energy, has been given in Fig. 8. From Fig. 8, it can be observed that the total CSPP's scheduled energy is approximately equal for all operational strategies. On the other hand, the almost equal scheduled energy in different operational strategies causes different expected profit and financial risk, meaning that the CSPP's share in the target markets varies from case to case. As shown in Fig. 8, in the absence of the intraday market, the CSPP focuses on offering in the DA market, resulting in the highest share of the DA participation compared to other strategies, and accordingly, the lowest expected profit and

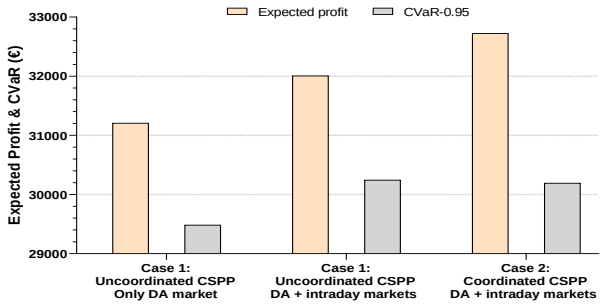

Fig. 7. Comparison of the CSPP's expected profit and CVaR in different operational strategies (risk-neutral state).

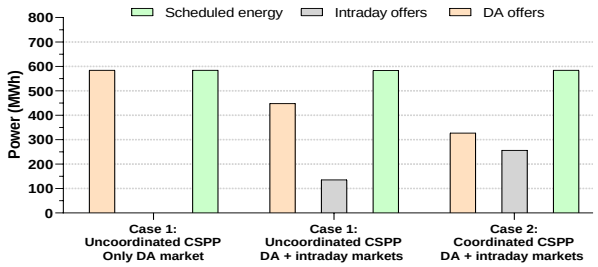

Fig. 8. Total DA, intraday, and scheduled offers of the CSPP in different operational strategies (risk-neutral state).

CVaR. By involving the intraday market in the uncoordinated operation, the DA's participation share is reduced. Afterward, the coordinated operation boosts the CSPP's intraday share, and consequently, its DA share is lessened. In summary, the main reason for the profitability of Case 2 is that the joint configuration enhances the HPP's flexibility for offering in the DA and intraday markets through giving a higher degree of freedom.

Fig. 9 illustrates the energy stored in the CSPP's thermal energy storage for various operational modes. As can be seen from this figure, except for the early hours, the stored energy of the thermal energy storage in Case 2 is higher than other strategies. It is observed in Fig. 9 that during the early hours, i.e., hours 1-6, the zero thermal production of the solar field and low energy prices are the reasons for not experiencing any fluctuations in the level of the stored energy in the thermal energy storage. During hours 7-20, the thermal energy storage is charged due to available thermal energy in the solar field. On the other hand, thermal energy storage is discharged during the last hours of the day as a result of having higher market prices. Eventually, on account of enforcing constraint (20), the level of the stored energy in the last period of the trading horizon would be equal to its corresponding value in the first period.

C. Impact of different configurations on the participation of the system in the DA and intraday markets

Fig. 10 and Fig. 11 present the expected offers of the CSPP, CAES unit, and wind farm in DA and intraday markets, respectively. As shown in Fig. 10, the DA offers of the CAES unit in both configurations for all trading periods except 9:00 p.m. are similar. Also, the wind farm's DA energy offers in the joint configuration for most hours are greater than the disjoint one, indicating a higher degree of freedom for the participation

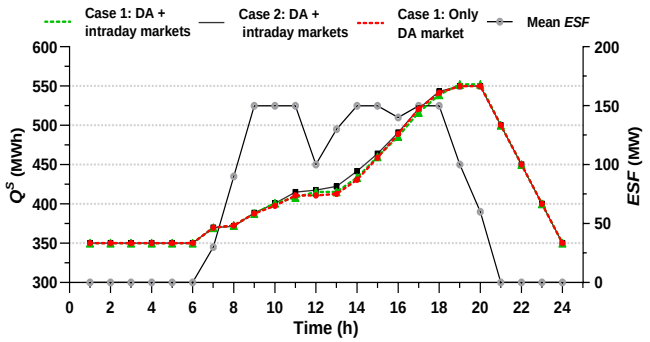

Fig. 9. Comparison of the energy stored in the CSPP's thermal energy storage in different operational strategies (risk-neutral state).

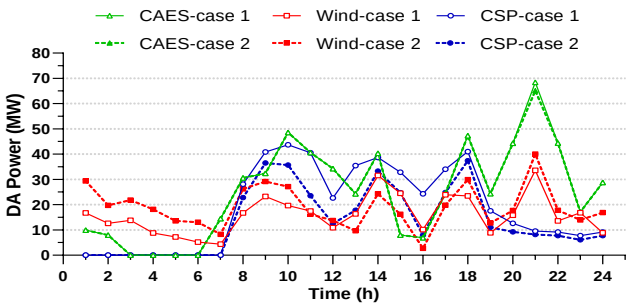

Fig. 10. Expected DA participation of the system in joint and disjoint configurations (risk-neutral state).

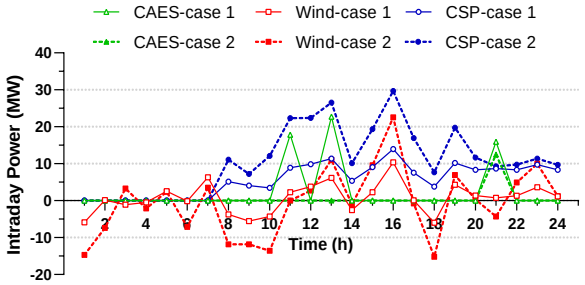

Fig. 11. Expected intraday participation of the system in joint and disjoint configurations (risk-neutral state).

of the wind farm in the this market. Another critical issue is that in the coordinated operation, the CSPP's DA energy offers are reduced compared to the disjoint configuration. This matter follows from the fact that in the joint configuration, the CSPP devotes a more portion of its generating capacity for selling energy in the intraday market, as shown in Fig. 11. Therefore, the coordinated operation leads to higher levels of CSPP's intraday energy offers for almost all periods in comparison with the uncoordinated one, except early hours in which the CSPP is offline for both configurations.

A Comparison between the intraday strategy of the wind farm in both configurations allows us to deduce that wind farm in Case 2 concentrates more on purchasing energy rather than selling it. This approach helps the HPP to manage its deviation in the balancing market more efficiently. Moreover, according to Fig. 11, the CAES unit participation in the intraday market is reduced from three hours to one hour by shifting from a

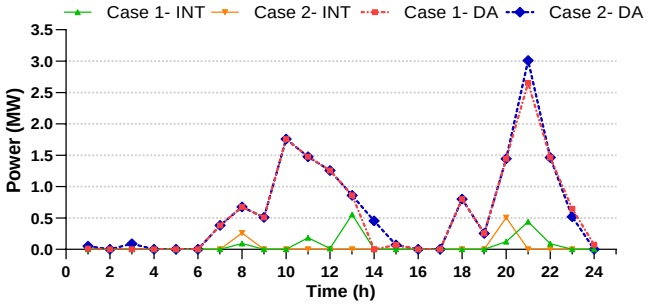

Fig. 12. Expected DRP's participation in DA and intraday markets for joint and disjoint configurations (risk-neutral state).

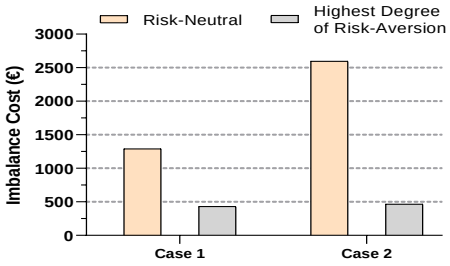

Fig. 13. Total expected imbalance cost incurred to the system in joint and disjoint configurations.

disjoint configuration to the joint one. Lastly, the total expected DRP's participation in the DA and intraday markets for Case 1 and Case 2 are illustrated in Fig. 12. According to Fig. 12, the total expected DA involvement of the DRP in the joint configuration is greater than the disjoint one, while with the intraday market, the opposite is the case. The reason lies in the fact that, by moving from Case 1 towards Case 2, the DRP reduces a portion of its intraday energy offers and devotes this portion to its participation in the DA market, hoping to let other HPP's elements to have greater involvement in the intraday market, as expressed in equation (36).

D. Impact of different configurations on the imbalance cost

The final investigation of this paper dedicates to the influence of the joint configuration on the imbalance cost. The comparison of the system's imbalance cost in two cases, including the risk-neutral state and an attitude with the highest degree of risk-aversion, has been depicted in Fig. 13. A comparison between the obtained results allows concluding that for both risk-free and conservatism approaches, the imbalance cost of the coordinated operation is greater. The principal reason is that the HPP tends to have more energy deviations in the balancing market in the hope of gaining a greater profit.

VI. Conclusion

This paper proposed a novel optimal behavior for an HPP containing a CSPP, a CAES facility, a wind farm, and a DRP in DA and intraday markets. The optimal behavior was organized and formulated as a bi-objective optimization problem based on the joint configuration of all existing resources, whereas the ϵ-constraint and lexicographic methods were exploited to find the Pareto solutions. The proposed optimal behavior in

DA and intraday markets was tested in two case studies. The key conclusions could be drawn as: 1) The joint exploitation of ϵ-constraint and lexicographic methods enhanced the performance of the CVaR-based optimal offering and bidding strategy problems in terms of obtaining equally spaced Pareto points in comparison with the conventionally used method, i.e., weighted-sum. Furthermore, compared to the weighted-sum approach, the proposed methodology was capable of deriving better solutions for the risk-neutral state as well as the case with the highest degree of risk-aversion. 2) The joint configuration brought substantial improvements in terms of both expected profit and CVaR compared to the disjoint one. 3) Incorporating the intraday offering into the conventional DA trading models not only raised the CSPP's profit but also reduced its related risk. 4) The joint configuration allowed all of HPP's elements to act more freely in DA and intraday markets, especially the CSPP and wind farm. Concretely, by moving from a disjoint configuration towards the joint one, the CSPP's intraday energy offers were increased, while its DA energy offers were diminished. In contrast, the wind farm concentrated more on purchasing energy from the intraday market, whereas increasing its offering packages in the DA market. 5) The joint configuration imposed a greater imbalance cost to the system compared to the disjoint one. Meanwhile, adopting suitable conservative strategies could be effectively employed to diminish the imbalance cost.

The authors' future research endeavor will concentrate on: 1) incorporating the offering and bidding strategy of the proposed HPP in the balancing market, whereas it acts in the role of a price-maker agent in this market; and 2) addressing the correlation among various uncertainty sources considered in this paper.

References

[1] J. Ji, H. Tang, and P. Jin, "Economic potential to develop concentrating solar power in China: A provincial assessment," *Renew. Sustain. Energy Rev.*, vol. 114, p. 109279, 2019.

[2] R. Sioshansi and P. Denholm, "The value of concentrating solar power and thermal energy storage," *IEEE Trans. Sustain. Energy*, vol. 1, no. 3, pp. 173-183, 2010.

[3] M. Petrollese, D. Cocco, G. Cau, and E. Cogliani, "Comparison of three different approaches for the optimization of the CSP plant scheduling," *Sol. Energy*, vol. 150, pp. 463-476, 2017.

[4] R. Dominguez, L. Baringo, and A. J. Conejo, "Optimal offering strategy for a concentrating solar power plant," *Appl. Energy*, vol. 98, pp. 316-325, 2012.

[5] G. He, Q. Chen, C. Kang, and Q. Xia, "Optimal Offering Strategy for Concentrating Solar Power Plants in Joint Energy, Reserve and Regulation Markets," *IEEE Trans. Sustain. Energy*, vol. 7, no. 3, pp. 1245-1254, 2016.

[6] D. Yu, A. G. Ebadi, K. Jermsittiparsert, N. H. Jabarullah, M. V. Vasiljeva, and S. Nojavan, "Risk-constrained Stochastic Optimization of a Concentrating Solar Power Plant," *IEEE Trans. Sustain. Energy*, 2019.

[7] H. M. I. Pousinho, J. Contreras, P. Pinson, and V. M. F. Mendes, "Robust optimisation for self-scheduling and bidding strategies of hybrid CSP-fossil power plants," *Int. J. Electr. Power Energy Syst.*, vol. 67, pp. 639–650, 2015.

[8] M. K. AlAshery, D. Xiao, and W. Qiao, "Second-Order Stochastic Dominance Constraints for Risk Management of a Wind Power Producer's Optimal Bidding Strategy," *IEEE Trans. Sustain. Energy*, 2019.

[9] J. Aghaei, M. Barani, M. Shafie-Khah, A. A. Sanchez De La Nieta, and J. P. S. Catalao, "Risk-Constrained Offering Strategy for Aggregated Hybrid Power Plant Including Wind Power Producer and Demand Response Provider," *IEEE Trans. Sustain. Energy*, vol. 7, no. 2, pp. 513–525, 2016.

[10] H. Khaloie et al., "Coordinated wind-thermal-energy storage offering strategy in energy and spinning reserve markets using a multi-stage model," *Appl. Energy*, vol. 259, p. 114168, 2020.

[11] H. Khaloie et al., "Co-optimized bidding strategy of an integrated wind-thermal-photovoltaic system in deregulated electricity market under uncertainties," *J. Clean. Prod.*, vol. 242, p. 118434, 2020.

[12] M. E. Nazari and M. M. Ardehali, "Optimal bidding strategy for a GENCO in day-ahead energy and spinning reserve markets with considerations for coordinated wind-pumped storage-thermal system and CO2 emission," *Energy Strateg. Rev.*, vol. 26, p. 100405, 2019.

[13] M. E. Nazari and M. M. Ardehali, "Optimal coordination of renewable wind and pumped storage with thermal power generation for maximizing economic profit with considerations for environmental emission based on newly developed heuristic optimization algorithm," *J. Renew. Sustain. Energy*, vol. 8, no. 6, p. 65905, 2016.

[14] R. Khatami, K. Oikonomou, and M. Parvania, "Look-Ahead Optimal Participation of Compressed Air Energy Storage in Day-ahead and Real-time Markets," *IEEE Trans. Sustain. Energy*, 2019.

[15] S. Shafiee, H. Zareipour, A. M. Knight, N. Amjady, and B. Mohammadi-Ivatloo, "Risk-Constrained Bidding and Offering Strategy for a Merchant Compressed Air Energy Storage Plant," *IEEE Trans. Power Syst.*, vol. 32, no. 2, pp. 946-957, 2017.

[16] S. Ghavidel, M. J. Ghadi, A. Azizivahed, J. Aghaei, L. Li, and J. Zhang, "Risk-Constrained Bidding Strategy for a Joint Operation of Wind Power and CAES Aggregators," *IEEE Trans. Sustain. Energy*, 2020.

[17] A. Attarha, N. Amjady, S. Dehghan, and B. Vatani, "Adaptive robust self-scheduling for a wind producer with compressed air energy storage," *IEEE Trans. Sustain. Energy*, vol. 9, no. 4, pp. 1659–1671, 2018.

[18] M. Di Somma, G. Graditi, and P. Siano, "Optimal Bidding Strategy for a DER Aggregator in the Day-Ahead Market in the Presence of Demand Flexibility," *IEEE Trans. Ind. Electron.*, vol. 66, no. 2, pp. 1509-1519, 2018.

[19] H. Golmohamadi, R. Keypour, B. Bak-Jensen, J. R. Pillai, and M. H. Khooban, "Robust Self-Scheduling of Operational Processes for Industrial Demand Response Aggregators," *IEEE Trans. Ind. Electron.*, vol. 67, no. 2, pp. 1387-1395, 2019.

[20] Y. C. Li and S. H. Hong, "Real-Time Demand Bidding for Energy Management in Discrete Manufacturing Facilities," *IEEE Trans. Ind. Electron.*, vol. 64, no. 1, pp. 739-749, 2017.

[21] Y. Wang, X. Ai, Z. Tan, L. Yan, and S. Liu, "Interactive dispatch modes and bidding strategy of multiple virtual power plants based on demand response and game theory," *IEEE Trans. Smart Grid*, vol. 7, no. 1, pp. 510–519, 2015.

[22] N. Hajibandeh et al., "Demand Response-Based Operation Model in Electricity Markets With High Wind Power Penetration," *IEEE Trans. Sustain. Energy*, 2019.

[23] L. P. Garcés and A. J. Conejo, "Weekly self-scheduling, forward contracting, and offering strategy for a producer," *IEEE Trans. Power Syst.*, vol. 25, no. 2, pp. 657–666, 2010.

[24] J. M. Morales, A. J. Conejo, and J. Pérez-Ruiz, "Short-term trading for a wind power producer," *IEEE Trans. Power Syst.*, vol. 25, no. 1, pp. 554–564, 2010.

[25] A. J. Conejo, M. Carrión, and J. M. Morales, *Decision Making Under Uncertainty in Electricity Markets*, vol. 1. Boston, MA: Springer US, 2010.

[26] G. Chiandussi, M. Codegone, S. Ferrero, and F. E. Varesio, "Comparison of multi-objective optimization methodologies for engineering applications," *Comput. Math. with Appl.*, vol. 63, no. 5, pp. 912–942, 2012.

[27] S. Shafiee, H. Zareipour, and A. Knight, "Considering Thermodynamic Characteristics of a CAES Facility in Self-scheduling in Energy and Reserve Markets," *IEEE Trans. Smart Grid*, vol. 3053, no. d, pp. 1–1, 2016.

[28] B. McGrail et al., "Technoeconomic performance evaluation of compressed air energy storage in the Pacific Northwest," *Pacific Northwest Natl. Lab. Richland*, USA, 2013.

[29] A. Jamali et al., "Self-scheduling approach to coordinating wind power producers with energy storage and demand response," *IEEE Trans. Sustain. Energy*, 2019.

[30] "SCENRED2." [Online]. Available: https://www.gams.com/24.8/docs/tools/ scenred2/index.html. [Accessed: 05-Sep-2019].

[31] "Bienvenido | ESIOS electricidad - datos - transparencia." [Online]. Available: https://www.esios.ree.es/es. [Accessed: 14-Mar-2019].

[32] "Weather history meteoblue." [Online]. Available: https://www.meteoblue.com/en/historyplus. [Accessed: 22-Apr-2019].